ARMY RESEARCH LABORATORY

Modification of the Acoustic Spectrum of Detonation Tube Shock Waves by Timed Multiple-Pulse Addition

H. Edwin Boesch, Jr., Christian G. Reiff, and Bruce T. Benwell

ARL-TR-2203 May 2000

The findings in this report are not to be construed as an official Department of the Army position unless so designated by other authorized documents.

Citation of manufacturer's or trade names does not constitute an official endorsement or approval of the use thereof.

Destroy this report when it is no longer needed. Do not return it to the originator.

Army Research Laboratory

Adelphi, MD 20783-1197

ARL-TR-2203 **May 2000**

Modification of the Acoustic Spectrum of Detonation Tube Shock Waves by Timed Multiple-Pulse Addition

H. Edwin Boesch, Jr., Christian G. Reiff

Sensors and Electron Devices Directorate, ARL

Bruce T. Benwell

Directed Energy Technologies

Abstract

Detonation tubes are simple devices capable of producing substantial acoustic power that may be useful for the simulation of high-level acoustic environments. We report results of an investigation into the modification of the acoustic spectrum produced by detonation tubes by timed addition of the shock-wave outputs of six detonation tubes fired in sequence. We first examined the output of a single detonation tube as a function of range and found that it conformed to existing models for spherical blast waves when appropriate initial conditions were derived. We found timing schemes for the firing of the multiple tubes that (1) produce a substantial shift of the acoustic energy to lower frequencies by maximizing the duration of the positive pressure pulse, or (2) maximize the acoustic energy output in a narrow frequency range by matching the pulse-to-pulse delay to the total duration (positive and negative pressure phases) of a single detonation wave.

Contents

Figures

Table

1. Introduction

Detonation tubes (DTs) are conceptually simple devices that can repetitively and reliably produce acoustic energy at high intensities. These characteristics make detonation tubes attractive for applications that require substantial acoustic power from a compact source. However, the acoustic output of a single DT is not suitable for many applications, since the output is by nature impulsive or broadband rather than continuous. Also, the similarity characteristics of blast waves [1] ensure that the frequency content of the acoustic output of a single detonation tube is largely constrained by the energy of the shock-wave source and our range from it. In this report, we present the results of our initial experiments directed at exploring the means to generate impulsive acoustic energy with a modified frequency spectrum by timed and repetitive firing of an array of detonation tubes.

DTs produce pressure transients that have a shock profile that is typical of those produced by a wide range of shock-wave sources, including free-air explosions and gunfire at all scales. Further, such a shock profile is the primary component of pressure transients produced by transonic and supersonic flow associated with aeronautical structures, turbines, and rocket engines.

Typically, a DT consists of a cylinder closed at one end and open to atmosphere at the other, with a means for rapidly injecting and igniting an explosive mixture of a gaseous fuel and oxidizer. If the mixture is ignited at the closed end of the tube, a high-pressure detonation wave quickly forms in the mixture and propagates through the tube at a high Mach number and out the open end (muzzle) (fig. 1, top). In free air, the (initially) unipolar positive pressure pulse quickly converts to a bipolar

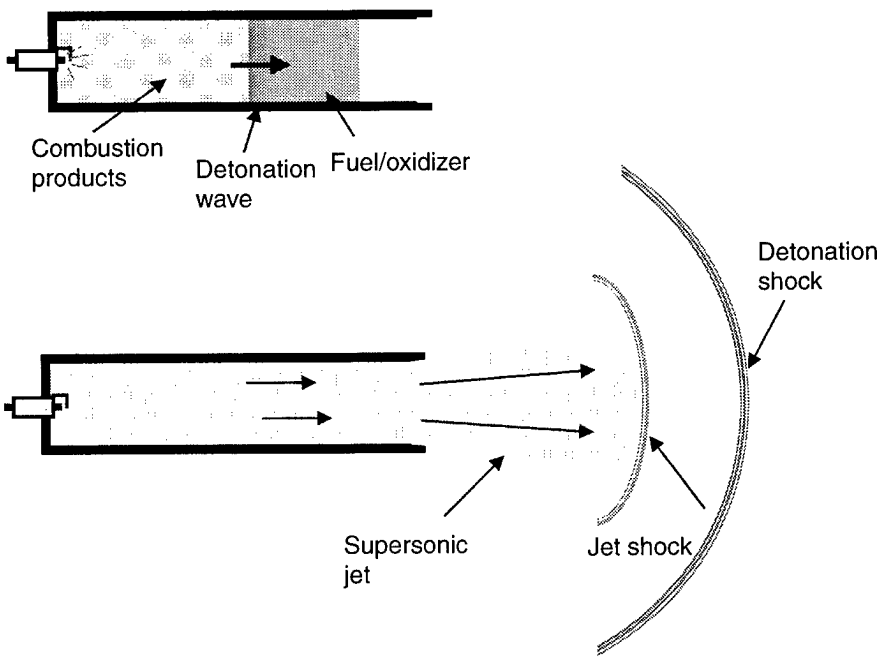

Figure 1. Schematic of secondary shock-wave formation by jet from DT.

shock-wave signature characterized by a rapid (within a few microseconds) rise to a positive peak, a pseudo-exponential fall to and through ambient atmospheric pressure, and a lower amplitude but longer duration negative pressure peak with a return to ambient pressure (see fig. 1). As noted, this pressure-time signature is general and applies to a wide range of shock-wave sources. For example, the signatures of a small-caliber gunshot and a large high-explosive detonation at comparable ranges differ primarily in the peak pressures reached in the (positive) overpressure and (negative) underpressure phases and in the duration of these pressure pulses. A useful approximation to this pressure-time signature is given by

$$p(t) = \Delta p\,(1 - t/t_+)\,(1 - t/\tau)\,(1 - (t/\tau)^2),\ 0 < t < \tau, \qquad (1)$$

where Δp is the magnitude of the peak positive pressure, t_+ is the duration of the positive pressure as measured at the ambient-pressure baseline, and τ is the total duration of the pressure transient, including both positive and negative phases [2]. For zero air particle velocity at the end of the pulse (linear, or *acoustic*, regime), τ is constrained to about $3.58t_+$. The waveform for this condition is shown in figure 2(a). The acoustic spectrum for an impulse with $t_+ = 1$ ms from Fourier analysis is shown in figure 2(b) and 2(c). The dominant acoustic frequency f_p for this pulse is ~238 Hz. Figure 2(d) shows the fractional integrated acoustic power (normalized watts per square meter) for this 1-ms pulse as a function of frequency. The median power frequency (the frequency at which the integral from zero frequency of the fractional acoustic power spectrum equals 0.5, also designated as the 50-percent cumulative power frequency—50% CPF) is ~297 Hz. A small DT at ranges of a few meters will typically produce an impulse with t_+ near 1 ms; therefore, much of the radiated acoustic energy from such a source is in the range of a few hundred hertz. The initial fast pressure rise contributes substantial energy in the high audible frequency range above 1 kHz; as shown in figure 2(c), these higher frequency components roll off at –20 dB per decade in frequency ($1/f$ spectrum).

For our applications, our goal was to shift the acoustic energy available from a DT source to lower audible frequencies (below 100 Hz) and to reduce the energy content in the range above 1 kHz, where the human ear is particularly susceptible to damage. Since the frequency content of the waveform produced by a single detonation tube is largely determined by its size and therefore not easily altered for devices constrained to a certain size range, we examined the possibility of synthesizing a waveform with the desired frequency content by adding the outputs of multiple DTs. In essence, we would fire several DTs in a predetermined rapid sequence into a common air volume to cause their waveforms to interact and generate a new waveform with altered characteristics.

If the tubes are close together (within a few tube diameters) and are fired so that their detonation waveforms overlap in time, the shock fronts from the tubes can interact at pressures in the medium shock regime (of the order of 100 kPa). The second (and all later) shock fronts do not propagate in the undisturbed ambient environment seen by the first shock, but in an

altered and highly dynamic environment. The shock waves in a series will then propagate at different velocities and their amplitudes are expected to add nonlinearly; so simple superposition of the detonation tube waveforms is not expected to hold. This shock-on-shock problem is not well understood; further development of the theory of such interactions is the subject of a companion paper [3]. Here we report the results of a limited experimental and theoretical study of the interaction of shock waves from multiple DTs.

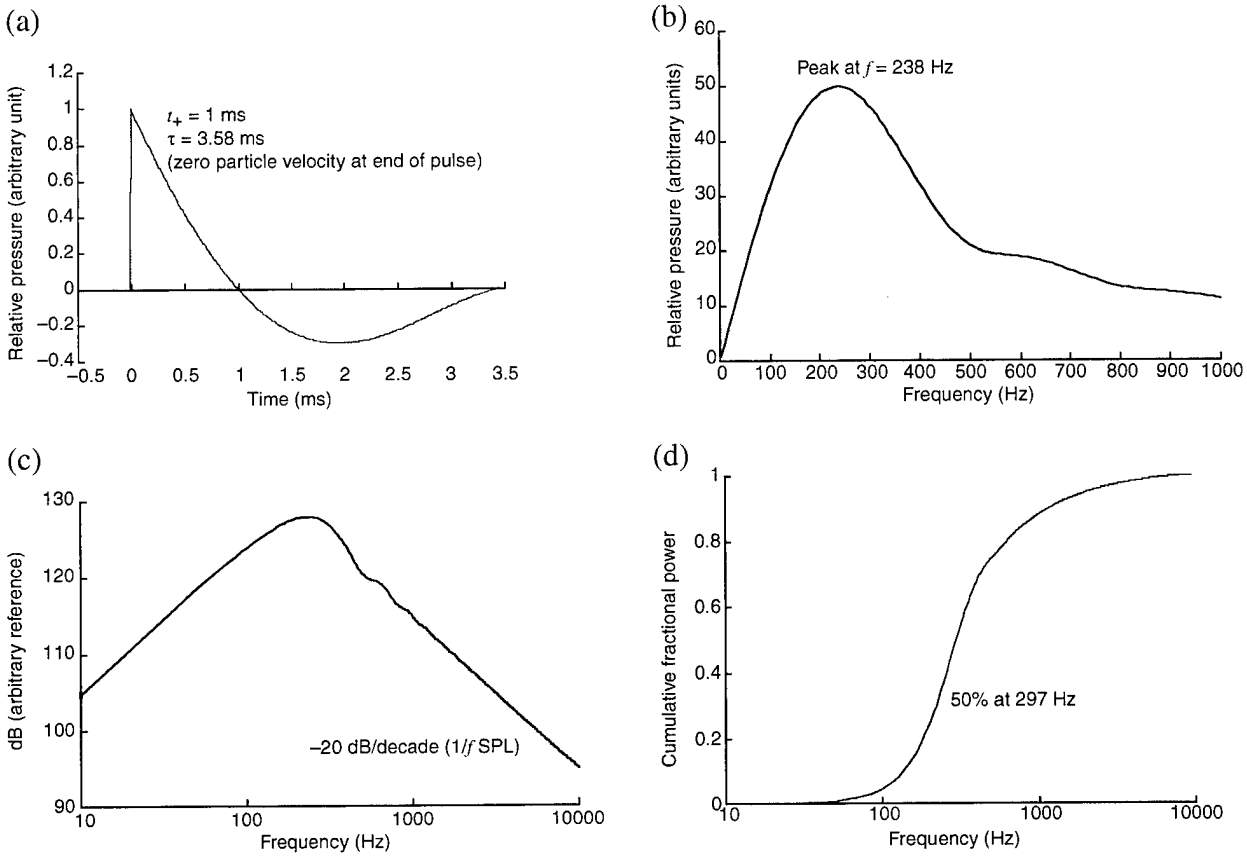

Figure 2. Idealized blast wave for t_+ = 1 ms, τ = 3.58 ms: (a) time history of SPL, $p(t)$; (b) low-frequency acoustic spectrum; (c) logarithmic acoustic spectrum; and (d) integrated fractional acoustic power as a function of frequency.

2. Addition of Ideal Blast Waves

Even in the acoustic or linear regime ($\Delta p << 100$ kPa), we cannot accurately calculate the waveform generated by the addition of signals from multiple impulsive acoustic sources by the simple addition of their amplitudes (linear superposition). If the sources produce substantial energy at frequencies f_p with corresponding wavelengths that are much greater than the distance between the sources, and the time delays between the firing of these sources are much less than $1/f_p$, the sources will interact with each other and emit acoustic energy into a radiation resistance (acoustic impedance of the atmosphere) that is effectively altered from its free-air value. The exact calculation of the resulting addition of waveforms from multiple interacting sources is beyond the scope of this report.

However, as a guide, we first examine the linear superposition of a series of ideal blast waves (eq (1)), using ($t_+ = 1$ ms, $\tau = 3.58$ ms) waveforms as an example (see fig. 1). An initial strategy for increasing the low-frequency content of the waveform produced by adding blast waves would be simply to *stretch* the effective duration of the summed pulses by delaying successive individual DT pulses just enough to prevent the instantaneous sound pressure level (SPL) $p(t)$ from going negative after the positive pressure phase from the previous pulse. We assume that the n waves are identical in time history and amplitude and are successively shifted in time with respect to each other by delay times Δt_i, where $i = 1, \ldots, n - 1$. Figure 3(a) shows the result for addition of five blast waves with $\Delta t_i = 1$ ms. Note in the figure that $p(t)$ repeatedly and increasingly goes negative following the second pulse as the lower amplitude but longer duration negative phases add in. Since the integral over τ of each of the individual pulses is zero, the integral of a linear summation of these pulses must also equate to zero. Consequently, a sufficiently long sequence of such pulses must reach a *steady state*, in which the positive and negative pressure phases average to zero, and pulse stretching must inevitably yield diminishing returns for large n. That is evident by pulse 4 for $\tau = 1$ ms. Figures 3(b) to 3(d) show the low-frequency linear and full-range logarithmic Fourier spectra and integrated power versus frequency calculated for this case. Compared to the benchmark single pulse (fig. 2), the longer duration of the five-pulse transient contributes some energy at lower frequencies (peak at ~100 Hz in fig. 3(b); compare to fig. 2(b)); however, the 50-percent CPF has dropped only slightly, from 297 Hz to 281 Hz (compare fig. 2(d) and 3(d)). Almost 25 percent of the acoustic energy in this five-pulse transient is now concentrated at the pulse repetition rate (1 kHz), and almost 40 percent of the total energy is at 1 kHz or higher.

Figure 4 shows results for five pulses with $\Delta t_i = 0.5$ ms. The pulses are close enough that $p(t)$ stays positive for over 2.5 ms. Again, the peak frequency (~159 Hz (fig. 4(b)) is associated with the total pulse duration. More importantly, the 50-percent CPF is now 171 Hz, and relatively little energy (<10%) is contributed by frequencies above 1 kHz.

Figure 5 shows results for five pulses with Δt_i chosen for each pulse to maximize the time that $p(t)$ remains at or above the baseline (Δt_i = 1.0, 0.65, 0.55, and 0.47 ms). The spectrum shows a strong dominant frequency near 134 Hz, and the 50-percent CPF is now 164 Hz. Less than 15 percent of the energy is above 1 kHz.

Overall, our modeling suggests that multiple-pulse addition could shift the acoustic energy of single DT pulses to substantially lower frequencies, and that a promising strategy for the addition is to prolong the initial positive $p(t)$ transient as much as possible without allowing zero crossings.

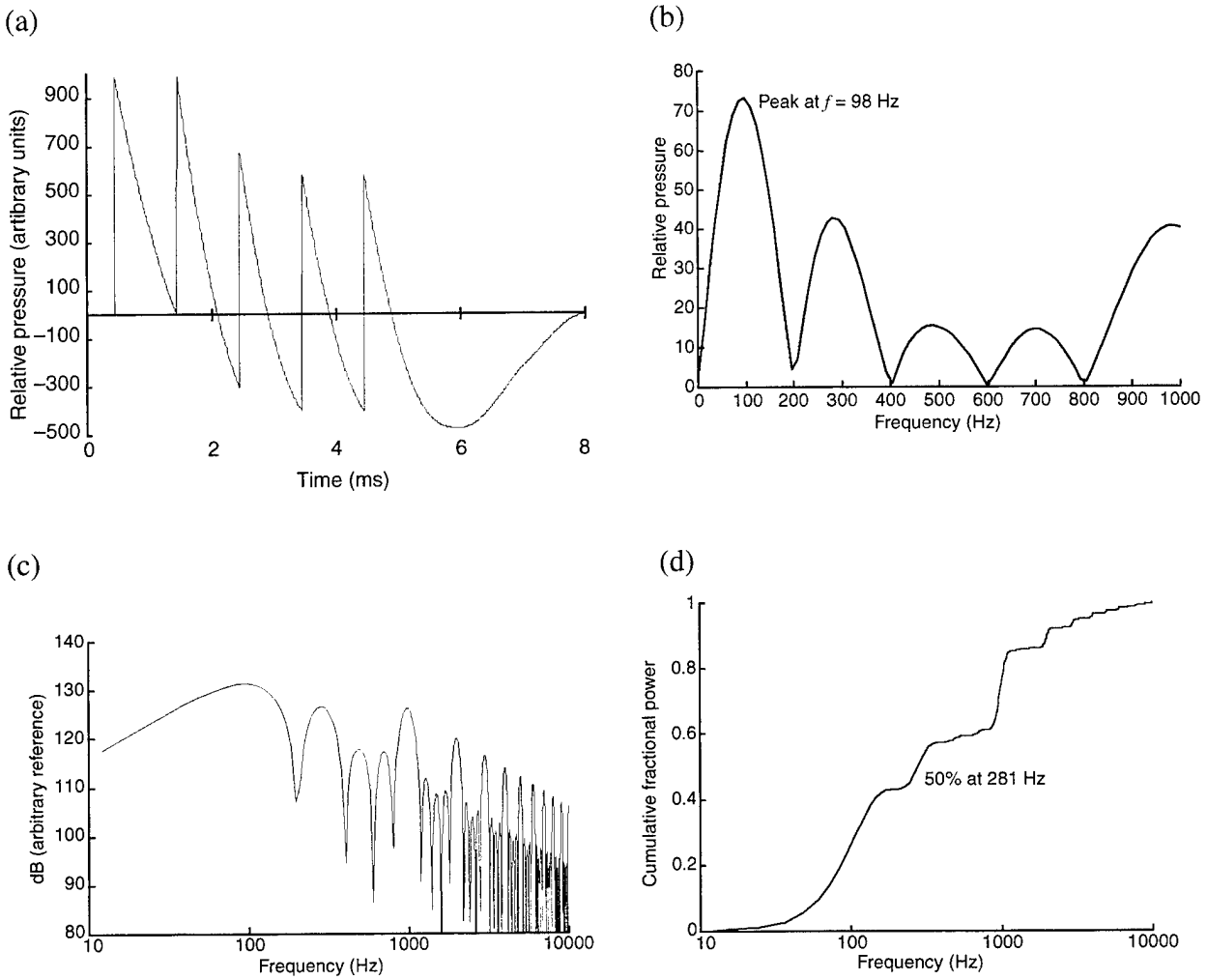

Figure 3. Linear superposition of five blast waves from figure 2 with delays of Δt_i = 1 ms: (a) time history of SPL, $p(t)$; (b) low-frequency acoustic spectrum; (c) logarithmic acoustic spectrum; and (d) integrated fractional acoustic power as a function of frequency.

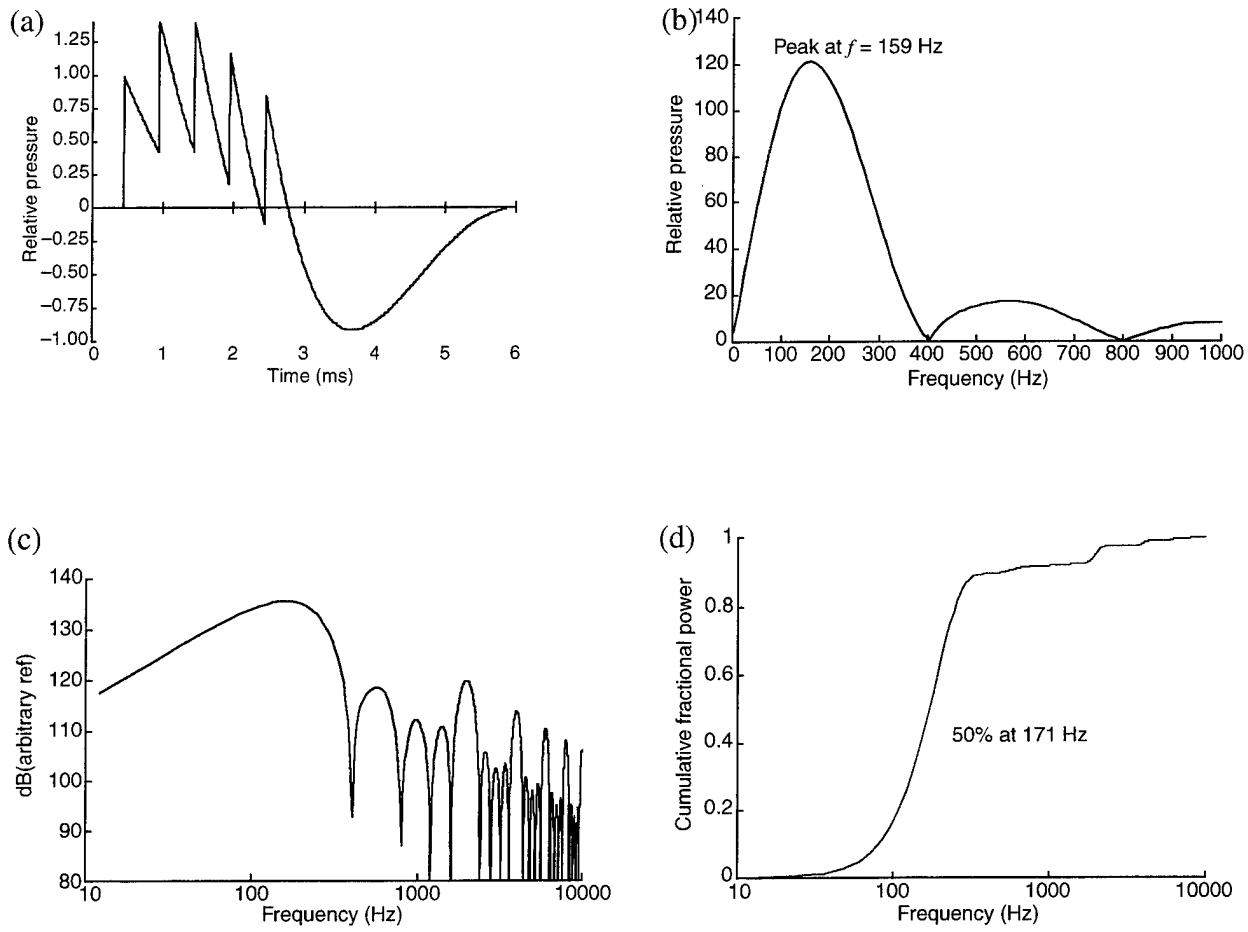

Figure 4. Linear superposition of five blast waves from figure 2 with delays of Δt_i = 0.5 ms: (a) time history of SPL, $p(t)$; (b) low-frequency acoustic spectrum; (c) logarithmic acoustic spectrum; and (d) integrated fractional acoustic power as a function of frequency.

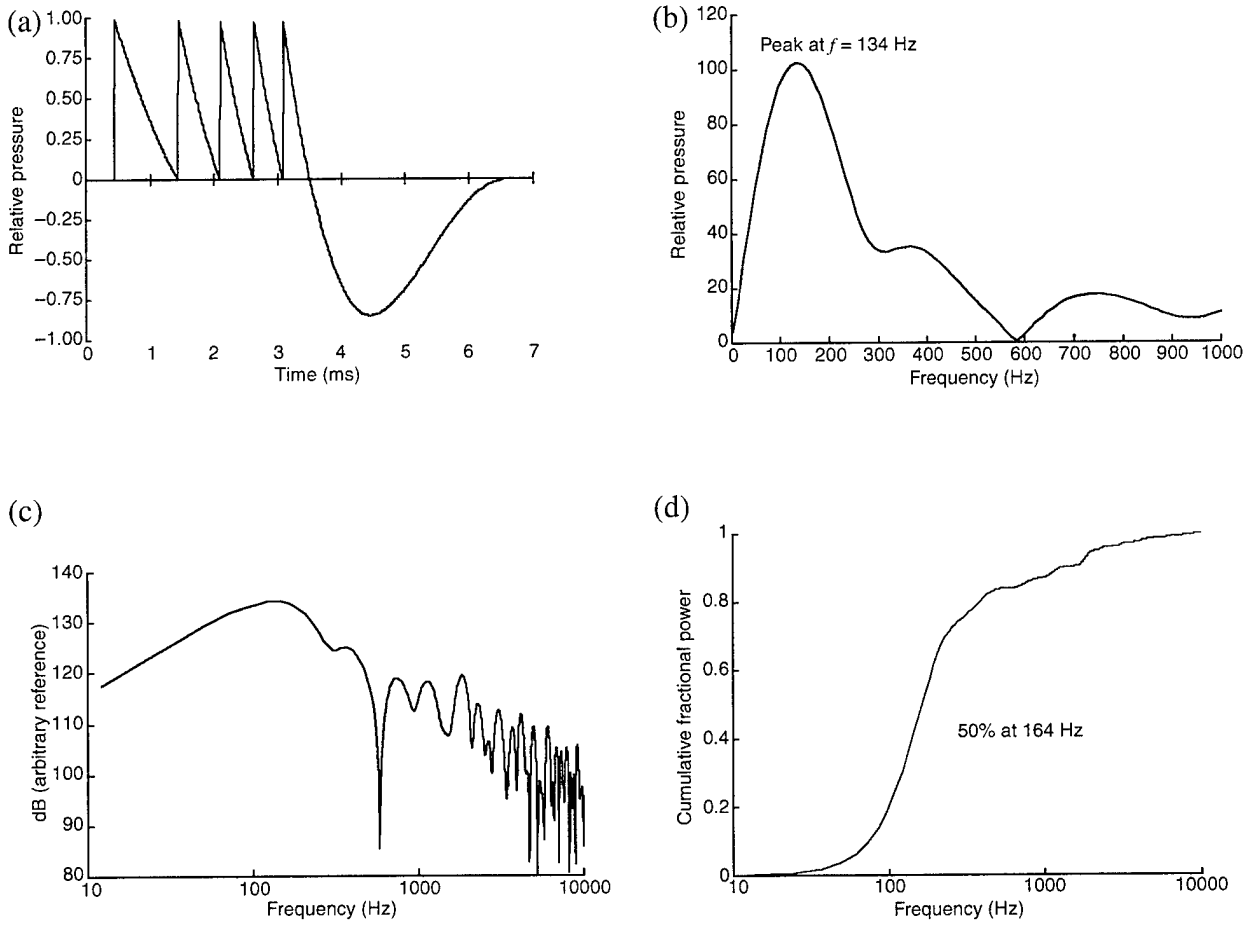

Figure 5. Linear superposition of five blast waves from figure 2 with delays Δt_i = 1.0, 0.65, 0.55, and 0.47 ms: (a) time history of SPL, $p(t)$; (b) low-frequency acoustic spectrum; (c) logarithmic acoustic spectrum; and (d) integrated fractional acoustic power as a function of frequency.

3. Experimental Setup

A simplified schematic of the experimental configuration is shown in figure 6. For most of the experiments described here, the DTs were cylinders with 6-in. interior diameters and length-to-diameter ratios greater than 4:1. The fuel and oxidizer were near-stoichiometric mixtures of ethylene and oxygen. These gases were rapidly injected into the tubes at the closed (breech) end and then ignited within a fraction of a second by an electric spark. The timing of the ignition for each tube could be individually controlled within 0.1 ms; variations in the ignition and detonation-wave formation processes resulted in tube-to-tube timing uncertainties of ±0.3 ms. Up to six DTs were arranged in an array, with their axes parallel and their open (muzzle) ends coplanar. The geometric center of the array at the muzzles was defined as *zero range*.

The experiments took place outdoors over lightly vegetated ground in a semi-arid environment. The axis of the DT array was approximately horizontal, with a height above the gently sloping ground of 1.5 m at the array and 2 m at a range of 15 m. We recorded the time history of the pressure waveforms from the array with blast probe pressure sensors and precision microphones located principally along the symmetry axis of the array. The blast probes were 12-in.-long, 1-in.-diam torpedo probes with side-mounted flush pressure transducers. PCB model 137A22 probes were used at short ranges (<1 m), and model 137A23 probes were used at longer ranges. Microphones were used at ranges of 5 m or greater: these were Bruel & Kjaer models 4136 or 4135 ¼-in. condenser microphones, with model 2669 preamplifiers and model 5935 power supplies. In addition, we recorded the pressure transients in the detonation tubes with PCB model 113A24 pressure transducers mounted near the muzzle; these signals served primarily as fiducial markers for each tube firing. We recorded the signals with a Tektronix TDS684A four-channel digital oscilloscope, an IOTech Wavebook/512 waveform digitizer operated by a laptop computer, and a Sony PC204A digital audio tape (DAT) recorder.

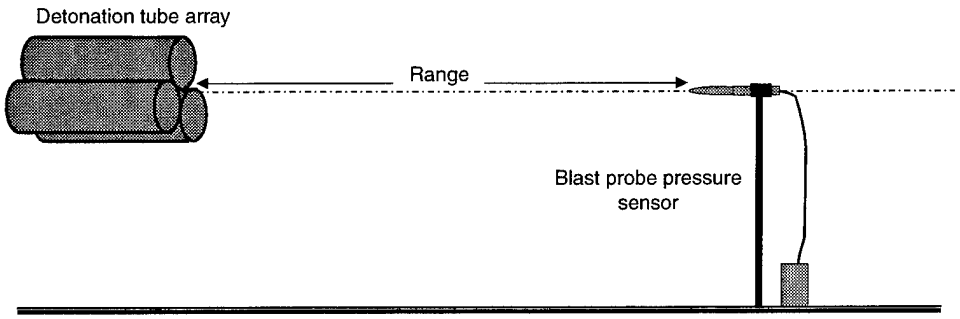

Figure 6. Schematic of experimental arrangement.

4. Single Tube Experiments

4.1 Results

Figures 7 and 8(a) show $p(t)$ waveforms recorded from the firing of a single DT. Waveforms are shown in each figure from two separate DT firings; the differences reflect minor pulse-to-pulse variations. For these figures, the blast probes were located on the tube axis at ranges of 0, 0.17, 0.29, 0.53, 0.95, and 5.0 m (fig. 7) and 15.24 m (fig. 8(a)). (All ranges are the distance from the muzzle of the DT to the pressure sensor on the side of the blast probe.) The waveform recorded at the muzzle of the DT (fig. 7(a)) shows the expected detonation transient interior to the tube: a peak positive pressure of over 2 MPa (about 300 psig) with a half-width of about 0.1 ms, a lower positive-pressure phase associated with the static combustion gas pressure behind the detonation wave, and a slow return to ambient pressure (blow-down) as these gases exit the tube. There is no negative-pressure phase in the tube on this time scale, since the tube is a net source of gas.

Figures 7(b) and 7(c) show $p(t)$ at 0.17 and 0.29 m from the tube (at about one and two tube diameters from the muzzle). In this range, the detonation wave is expanding roughly spherically into free atmosphere; the peak overpressure is dropping rapidly with range, a negative-pressure phase is developing, and the resulting duration t_+ of the positive pulse (as now measured to the negative-pressure crossover at the baseline) roughly doubles, from 0.22 to 0.48 ms. A delayed lower amplitude (near 100 kPa) positive-pressure peak appears just after the start of the negative phase (at about 0.7 ms in the figure). At 0.53 m (fig. 7(d)), the overpressure has dropped to about 110 kPa (near 1 atm), and a compensating negative phase is fully developed. The additional positive-pressure peak at about 1 ms with an amplitude near 70 kPa is now a major feature. This pattern is repeated at 0.95 m, 5 m (fig. 7(e) and 7(f)), and 15.24 m (50 ft) (fig. 8(a)). At 15.24 m, the overpressure has dropped to about 1 kPa (about 0.1 atm), and t_+ (not counting the secondary peak) has increased to about 1.2 ms.

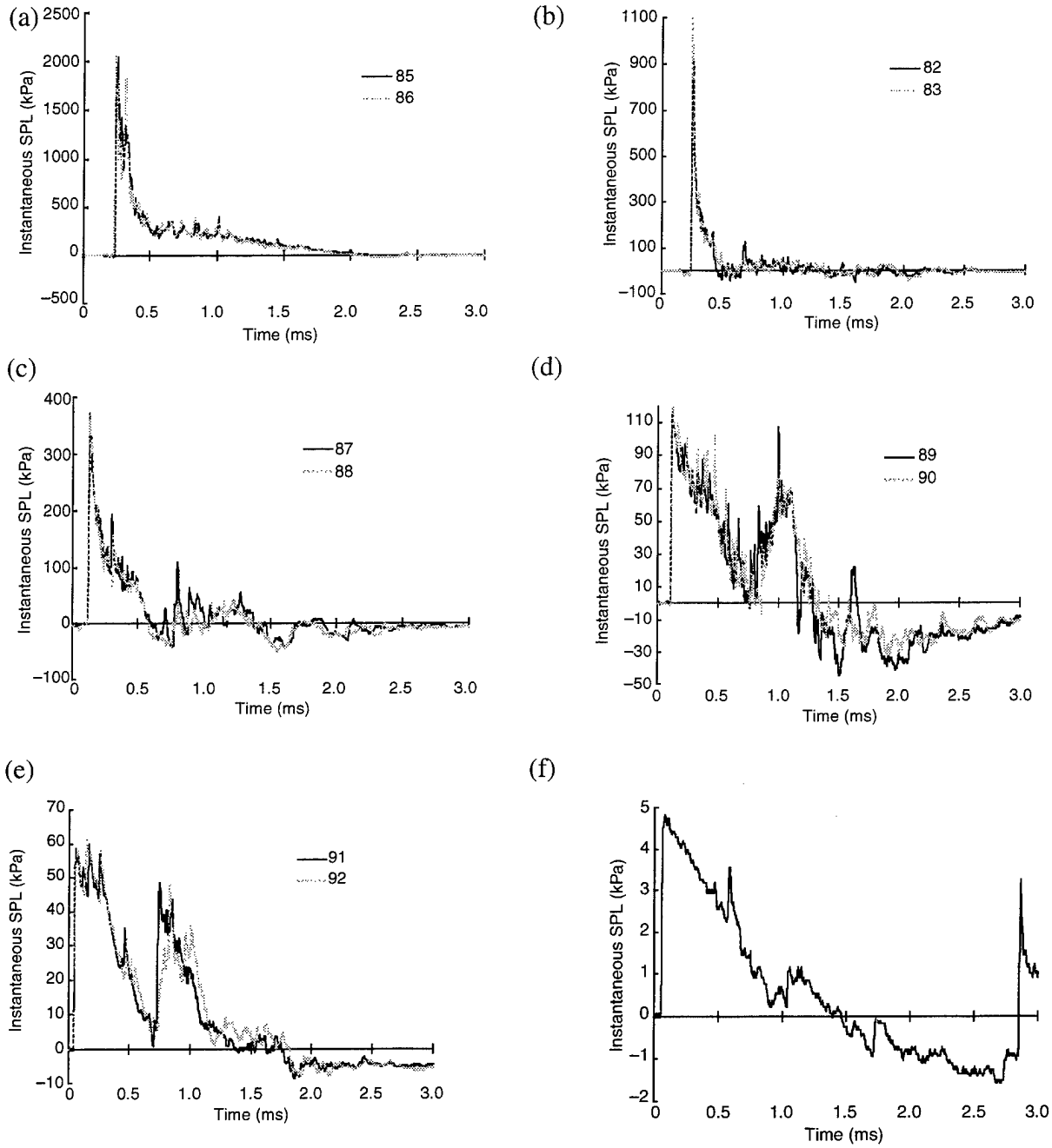

Figure 7. Time histories of SPL measured at various ranges r from a single DT: (a) r = 0.0 m, (b) r = 0.17 m, (c) r = 0.29 m, (d) r = 0.53 m, (e) r = 0.95 m, and (f) r = 5.0 m.

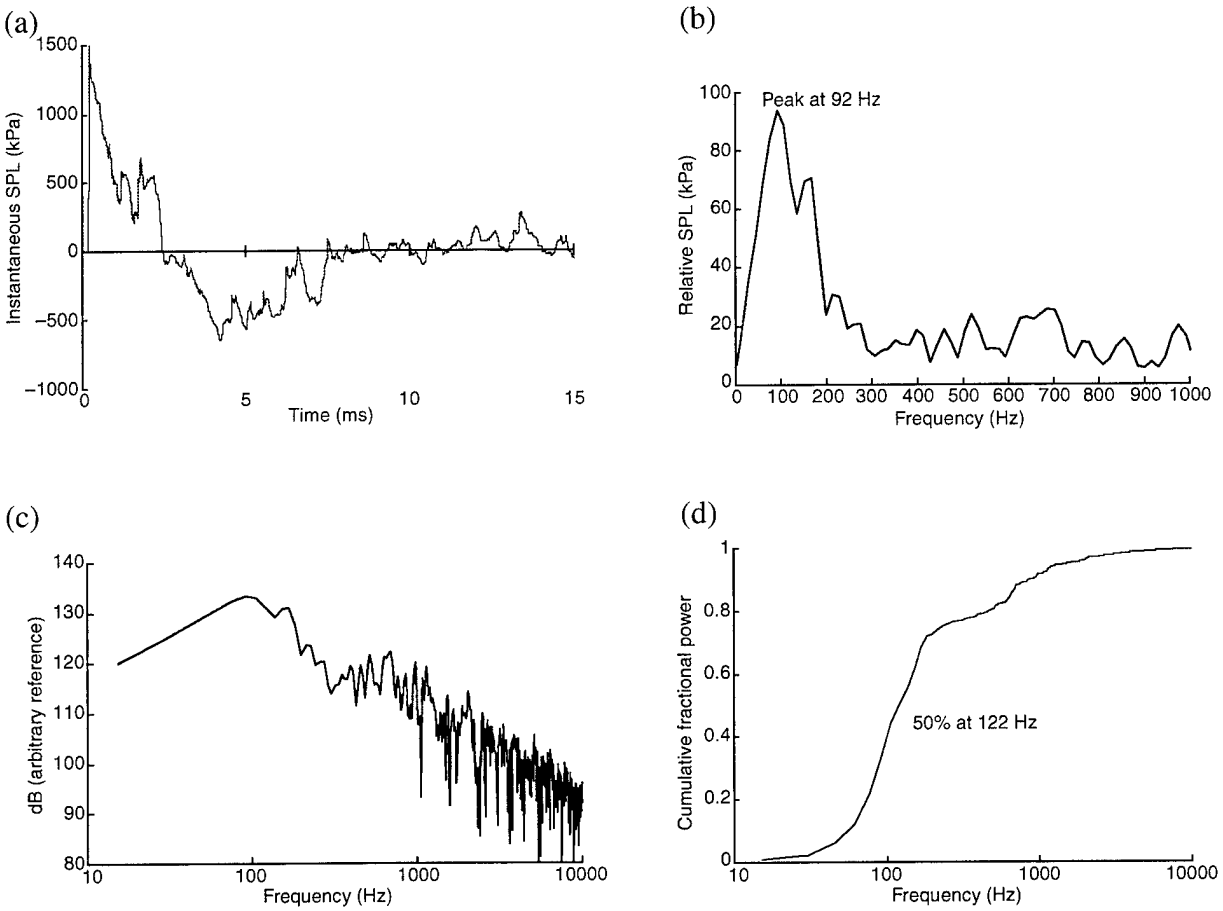

Figure 8. Pulse from a single DT measured at r = 15.24 m: (a) time history of SPL, $p(t)$; (b) low-frequency acoustic spectrum; (c) logarithmic acoustic spectrum; and (d) integrated fractional acoustic power as a function of frequency.

4.2 Discussion

In figure 9, we plot the measured initial positive peak overpressure Δp as a function of range from the data in figures 7 and 8(a). We also plot the magnitude of the second positive peak p_2 estimated from the figures. In figure 10, we plot the duration t_+ of the initial positive peak as estimated from the figures, excluding the contribution from p_2. Assuming a spherically symmetric blast in the intermediate to weak shock regime, Raspet [4] developed theoretical expressions for $p(r)$ and the duration t_s of the shock front near maximum overpressure based on the thickness of the compressed air shell at the shock front and its radial expansion rate. These expressions are

$$p(r) = \Delta p_0 \, (R_0/r) \, (1 + K \, (R_0/t_{s0}) \ln(r/R_0))^{-1/2} \tag{2}$$

and

$$t_s = t_{s0} \, (1 + K \, (R_0/t_{s0}) \ln(r/R_0))^{1/2} , \tag{3}$$

where R_0, t_{s0}, and Δp_0 are the equivalent spherical blast initial radius, peak overpressure duration, and pressure, and $K = (\gamma + 1)/(4\gamma c_0)$ is a constant ($\gamma = 1.4$ for air). Figure 9 is a plot of $p(r)$ (dashed smooth curve); the values of R_0 and t_{s0} were adjusted to 0.15 m and 0.01 ms, respectively, to produce a reasonable fit to the experimental results. The value of R_0 is physically reasonable, since 0.15 m is the diameter of the DT muzzle. We did not measure t_s directly; however, we expect t_+ to be proportional to t_s. The quantity $K_1 t_s$ is plotted in figure 10 (dashed smooth curve); K_1 was adjusted to the value 13.2 to produce a close fit to t_+. The fits of $p(r)$ and $K_1 t_s$ to the data are quite reasonable in this intermediate to weak shock regime.

The second positive-pressure peak, detectable at all ranges in figures 7 and 8(a) and plotted as p_2 in figure 9, is not a ground reflection. In our measurement geometry, ground reflections are delayed with respect to the direct wave by at least 6 ms at ranges under 1 m. In contrast to p, p_2 stays constant in magnitude with range from 0.17 to 0.53 m, where it becomes comparable to p and then falls off in roughly the same manner as p. An additional clue to the origin of p_2 is that this signal is either absent or strongly attenuated in measurements made at angles of more than 45° off the DT axis. We interpret p_2 as resulting from the blow-down of the DT following the detonation. Following the hypersonic passage of the detonation wave through and out of the DT, the high-pressure gas in the wake of the detonation wave begins to flow out of the tube. Upon entering the ambient atmosphere, the exhaust gas flow goes supersonic and forms a strong jet that is directed forward. The leading edge of this jet interacts with the ambient atmosphere to form a shock front (see fig. 1(b)). Since the jet is reasonably collimated, the jet shock front maintains intensity out to at least 0.5 m, in contrast to the leading detonation wave, which is expanding spherically.

At ranges of 0.53 and 0.95 m (fig. 7(d) and 7(e)), the contribution of p_2 to the total energy in the DT acoustic wave is clear; at greater ranges, the contribution is less obvious and must be distinguished from the primary

Figure 9. Range dependence of single DT overpressure characteristics. Solid line (squares) is measured initial positive overpressure Δp; dashed line is fit using equation (2). Dashed line (circles) is second overpressure p_2 attributed to jet.

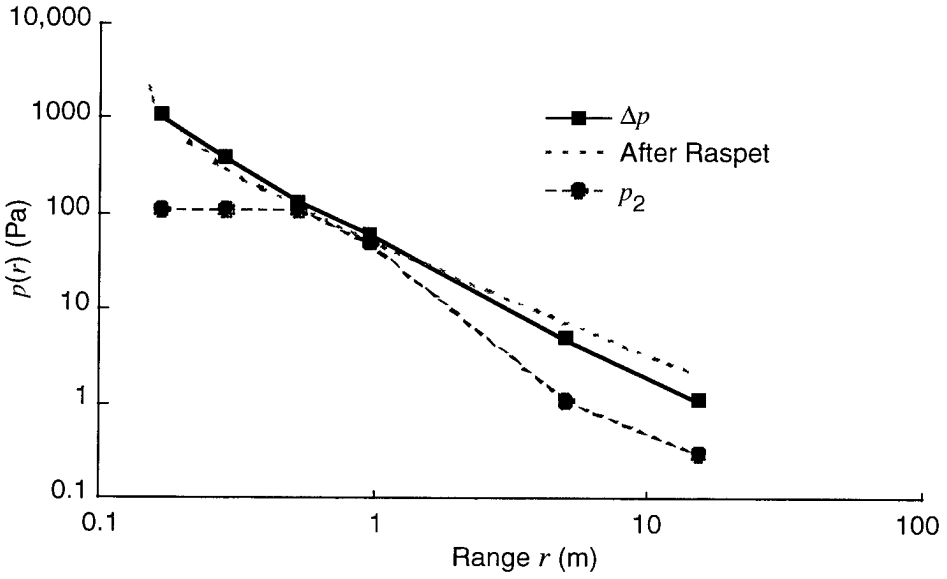

Figure 10. Range dependence of single DT overpressure pulse duration. Solid line (squares) is measured positive pulse duration t_+, and dashed line is scaled fit $K_1 t_s$ from equation (3). Solid curve (circles) is measured mean power frequency (50% CPF).

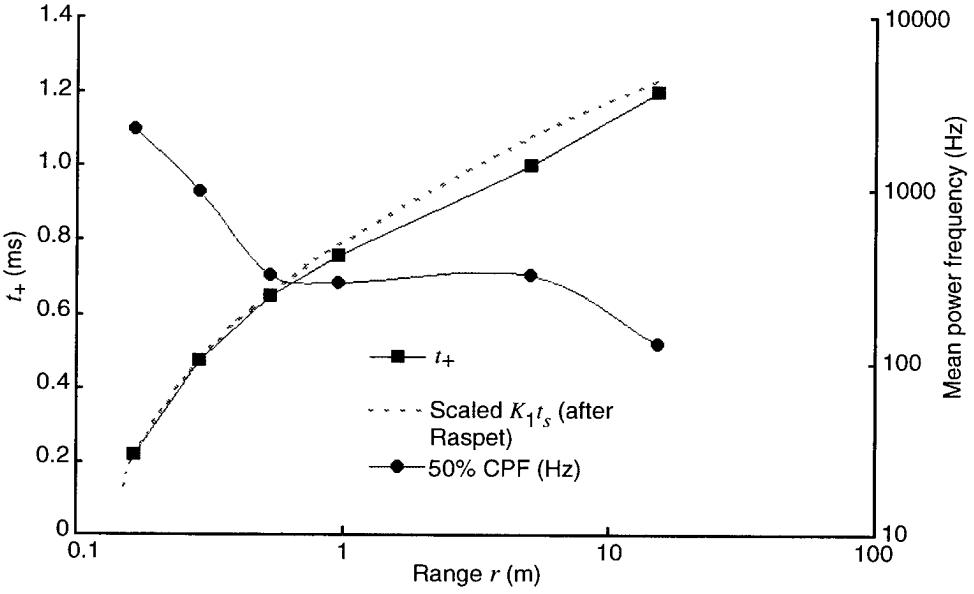

ground reflection. For our geometry, the ground reflection is expected to be delayed with respect to the direct wave by 2 to 4 ms at 5 m and 1 to 2 ms at 15.24 m. (The uncertainty results from variably sloped terrain on the measurement range.) The figures show the reflection arriving at 2.8 and 1.5 ms at 5 and 15.24 m, respectively. Particularly at these longer ranges, the reflection contributes substantially to the total energy in the acoustic signal.

Figures 8(c) and 8(d) show the logarithmic Fourier spectra and integrated acoustic power for the single DT pulses at 15.24 m. While this *real* pulse shows more frequency structure than the idealized pulse (compare to fig. 2), the overall characteristics are similar.

In addition to the measured pulse duration t_+, figure 10 also shows the 50% CPF values calculated from the measurements at the various ranges. The increasing pulse duration with range is the major contributor to the shift of the acoustic power spectrum to lower frequencies (atmospheric absorption plays only a minor role at these ranges at frequencies below 20 kHz). At 15.25 m (50 ft), the 50-percent CPF is down to 122 Hz from over 2 kHz at 0.165 m.

5. Multiple Tube Experiments

5.1 Simultaneous Firing of Six Tubes

Figure 11(a) shows the $p(t)$ waveforms recorded at 15.24 m (50 ft) produced by the firing of a single DT (lower dotted curve) and of six identical DTs (solid curve) simultaneously (within ±0.3 ms). Although the waveform recorded for the six-tube pulse at short range shows some sign of the individual DT pulses resulting from the timing variations, these individual pulses have coalesced into a single clean pulse plus the jet shock at the 15.25-m range. In addition to the normal pulse lengthening with range, this coalescence results from the tendency of the following shock waves to catch up with the leading shock waves when the shocks are close enough that the following shock is traveling in a high-pressure low-density region immediately behind the leading shock [3]. The initial overpressure Δp for the single and multiple pulses is about 1.4 and 2.6 kPa, respectively. Because of the simultaneity or coalescence of the DT pulses, the output of the six tubes is maximally coherent and, for a linear

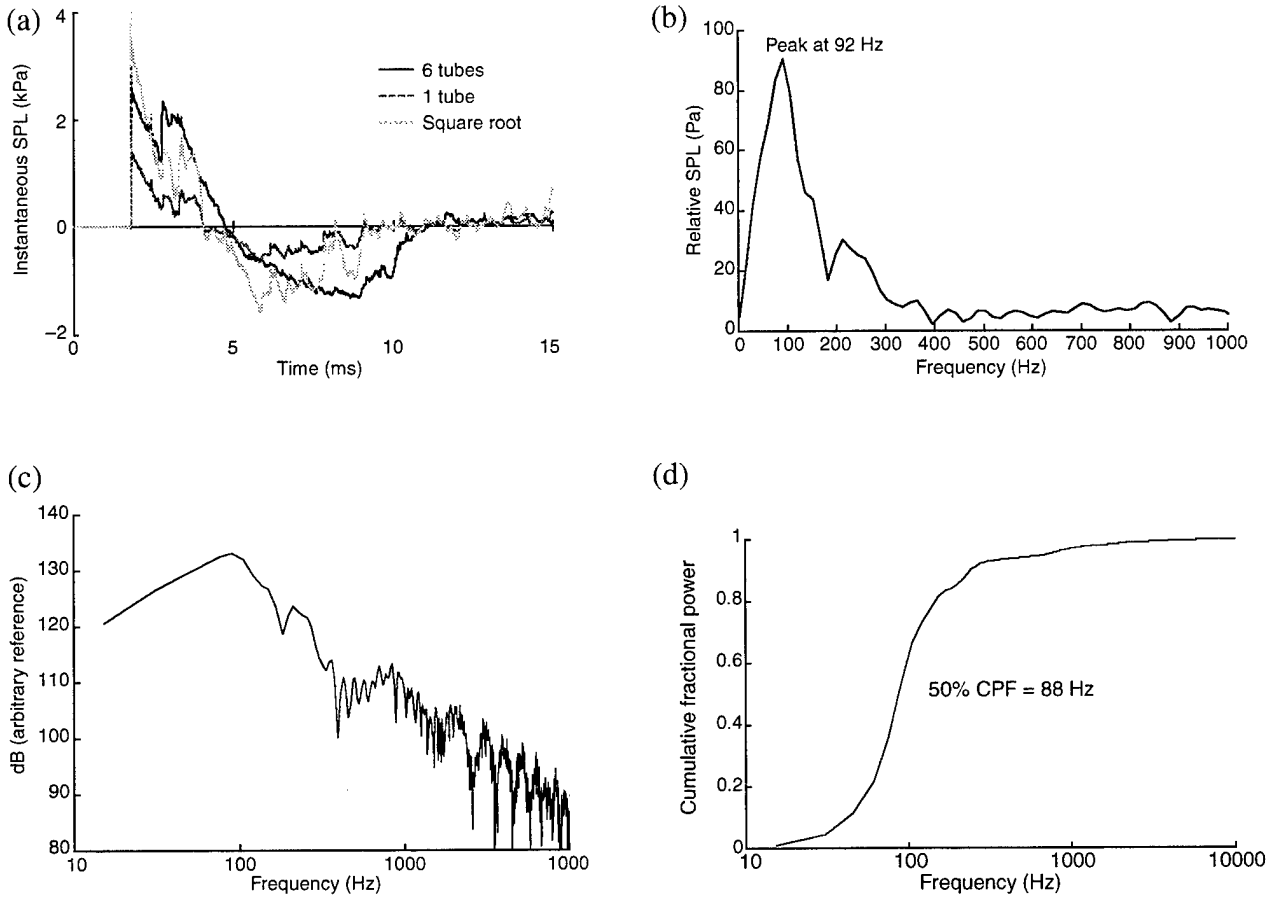

Figure 11. Pulse measured at 15.24 m from six DTs fired with Δt_i = 0 ms: (a) Time history of SPL, $p(t)$; for six DTs (solid curve), single DT (dashes), and $6^{1/2}p(t)_{1\ \text{tube}}$ (dotted curve); (b) low-frequency acoustic spectrum (six tubes); (c) logarithmic acoustic spectrum; and (d) integrated fractional acoustic power as a function of frequency.

interaction, we expect the resulting six-tube waveform to be that of the single tube at six times the power level (not six times the amplitude, or 36 times the power), as would be predicted by simple superposition of waveforms, or $p(t)_{6\ \text{tubes}} \sim 6^{1/2}\, p(t)_{1\ \text{tube}}$. As shown in the figure, the observed waveform differs from the $6^{1/2}\, p(t)_{1\ \text{tube}}$ curve with lower Δp amplitude, a longer pulse length, and a larger second peak (from the jet). These differences, or nonlinear effects, are attributable to increased pulse stretching because of the greater energy in the high-pressure shock interaction region close to the tubes and to an enhanced jet from the combined outputs of the tubes. The stretched pulse length results in a 50-percent CPF of about 90 Hz for the six-tube pulse (fig. 11(d)), which is substantially lower than the single-tube value of 122 Hz (fig. 8(d)).

5.2 Staggered Firing of Six Tubes

We then measured the acoustic output of the six tubes in the DT array with delays between tube firings of from 20 to 0.5 ms. Figures 12 and 13 show results for programmed uniform delays between tube firings of 8 and 2 ms, respectively.

With delays of 8 ms, the individual pulses are sufficiently separated in time that the sources do not interact substantially, and we expect that simple linear superposition of the pulses should apply. The dotted curve in figure 12(a) is the calculated $p(t)$ waveform for the linear addition of six identical pulses. The measured $p(t)$ shows somewhat reduced peak amplitudes, and the later pulses appear to be smeared out in time. We attribute this effect to transmission of the later pulses through a disturbed medium (turbulent hot gases) resulting from the exhaust jets from the DTs. Note that with 8-ms delays, the positive pulse from successive detonations arrives just as the negative phase from the preceding pulse is ending. Thus, 8 ms is the minimum delay for which the pulses add without overlap of negative and positive phases (without destructive interference). The resulting $p(t)$ in the figure may be described as a quasi-periodic waveform with superimposed high-frequency noise. At longer delays, the pulses become almost completely separated in time and are effectively independent.

Figure 12(b) shows the low-frequency fast Fourier transform (FFT) spectrum for this 8-ms delay. Note the large peak near 130 ± 8 Hz. (The frequency resolution for the FFT was 7.63 Hz.) This peak is attributable to the 8-ms repetition rate of the detonations and is also the apparent fundamental frequency of the synthesized quasi-periodic pressure wave. Below this peak are a series of peaks at ~22-Hz intervals; these frequencies may be associated with the roughly 45-ms duration of the entire pulse train. Above 1 kHz, the frequency spectrum shows the common overall –20 dB per decade roll-off (fig. 12(c)). The large step in the cumulative power curve for this pulse train (fig. 12(d)) results from the peak near 130 Hz; this peak accounts for almost two-thirds of the measured total acoustic power at 15.25 m from the source, and the 50-percent CPF is 126 Hz. Therefore, the six-pulse sequence with 8-ms delays actually has a higher mean frequency content than six tubes fired simultaneously (fig. 11(d)) or

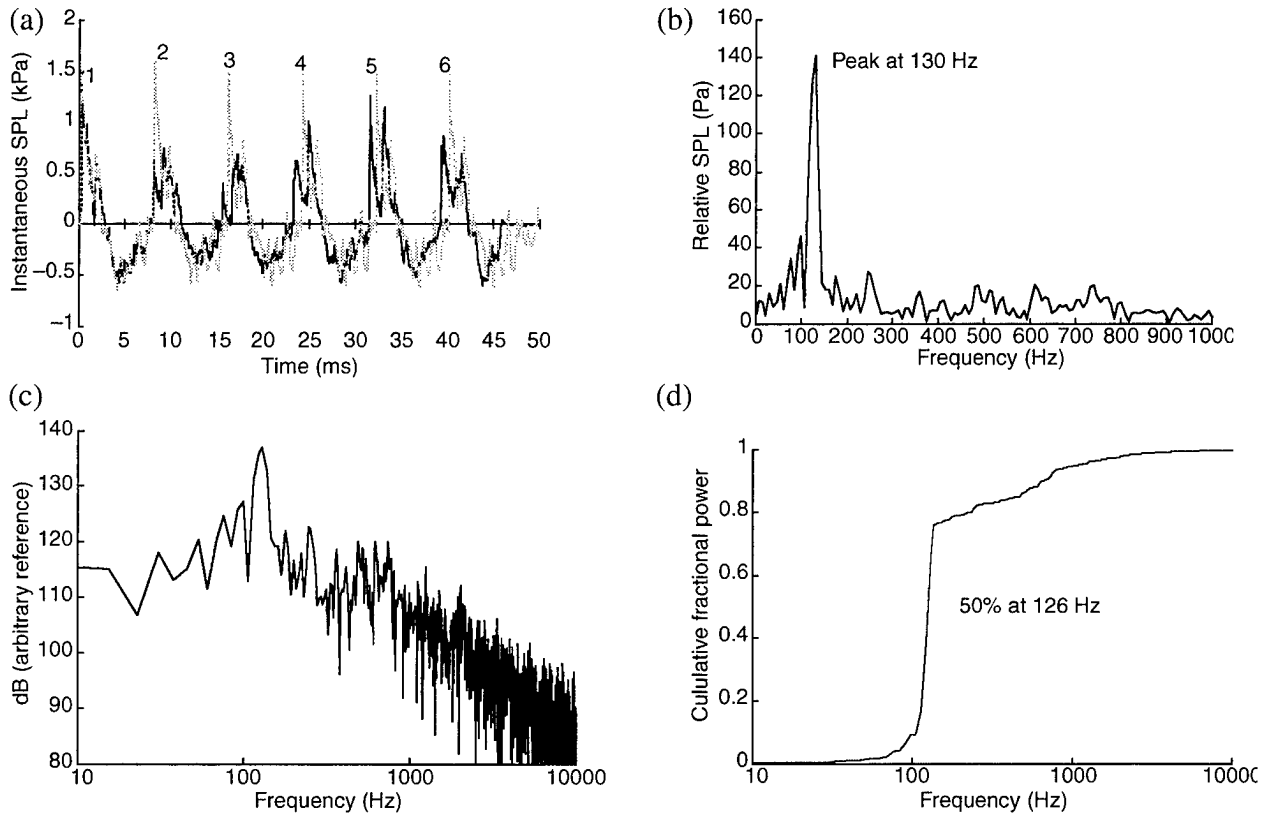

Figure 12. Pulse measured at 15.24 m from six DTs fired with Δt_i = 8 ms: (a) measured time history of SPL, $p(t)$ (solid curve), and calculated $p(t)$ based on single DT pulse (dotted curve); (b) measured low-frequency acoustic spectrum; (c) logarithmic acoustic spectrum; and (d) integrated fractional acoustic power as a function of frequency.

even a single tube (fig. 8(d)). However, the acoustic energy is strongly concentrated near a single frequency. Matching the pulse delays Δt to the duration τ of a single pulse may be an effective strategy for maximizing the acoustic power of a DT or other impulsive source at a single frequency. Since the pulse duration is a function of range for a shock-wave source, this matching should be done for a particular range and its associated τ.

Figure 13(a) shows recorded $p(t)$ (solid curve) for nominal delays of 2 ms between the six DT pulses. Again, the dotted curve in the figure is the calculated linear addition of six pulses. The actual measured delays varied by ~ ±0.2 ms; the delays in the simulation have been altered to match the measured values. In this sequence, successive pulses overlap in time. The first three pulses add in such a way that $p(t)$ is positive for the initial 4 ms. The later pulses swing both positive and negative. The overall behavior is reasonably well *predicted* for the earlier pulses by the linear addition calculation. One exception is pulse 3, which falls well below the calculated response. Other data suggest that this tube may have misfired. At later times, the predicted and observed responses match less well. As with the 8-ms pulse delays, the exhaust from the tubes may perturb these later pulses. The low-frequency spectrum produced by the 2-ms pulse burst is shown in figure 13(b). The roughly 10-ms duration of

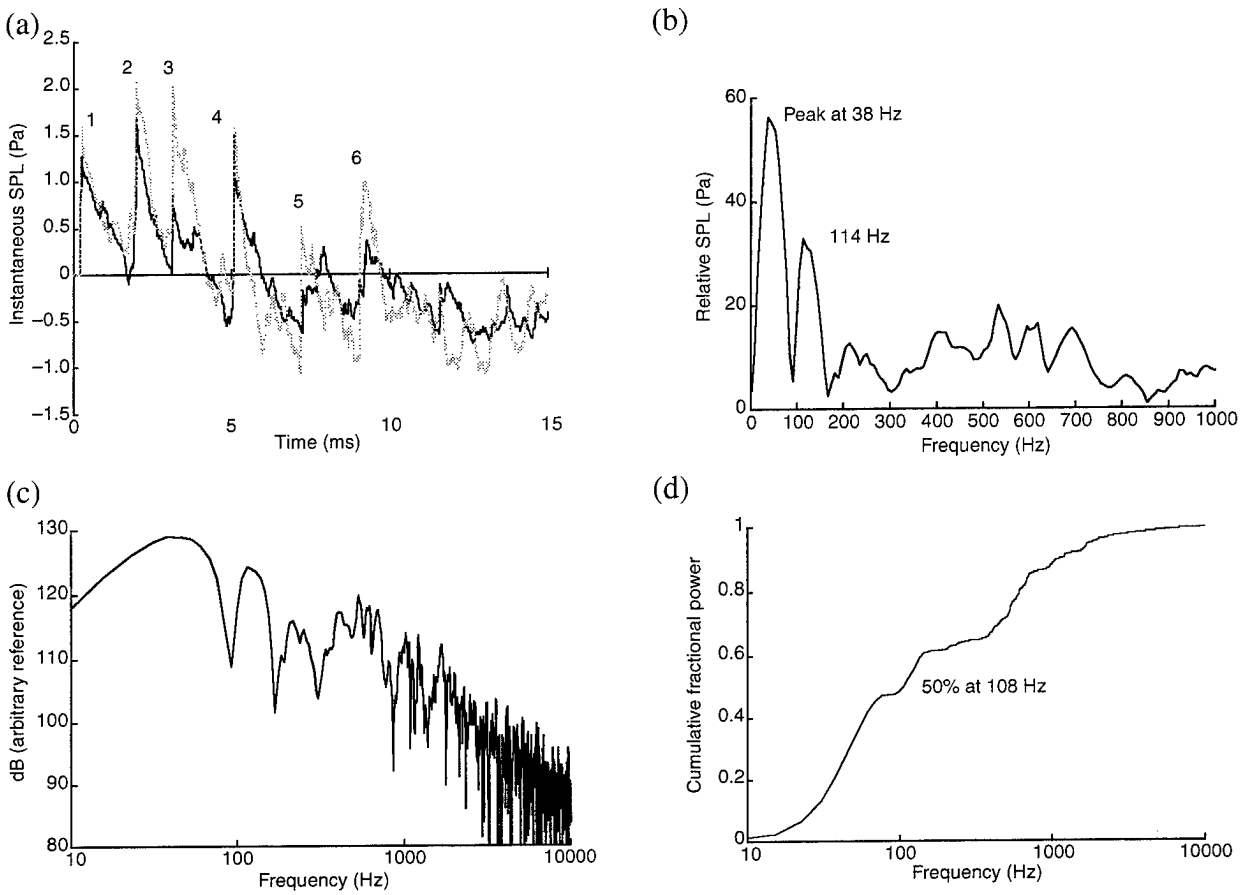

Figure 13. Pulse measured at 15.24 m from six DTs fired with Δt_i = 2 ms: (a) measured time history of SPL, $p(t)$ (solid curve), and calculated $p(t)$ based on single DT pulse (dotted curve); (b) low-frequency acoustic spectrum for measured $p(t)$; (c) logarithmic acoustic spectrum; and (d) integrated fractional acoustic power as a function of frequency.

the pulse train may account for the peak above 100 Hz; the (somewhat variable) 2-ms repeat interval is probably responsible for the broad hump in the spectrum around 500 Hz. The cause of the peak near 40 Hz, which implies a period near 25 ms, is not clear. The 50-percent CPF for this sequence is about 108 Hz; this value is lower than for the 8-ms sequence, but not as low as for the six-tube simultaneous-fire sequence, and the acoustic power is much more broadly distributed in frequency than for the 8-ms delays.

Figure 14(a) shows $p(t)$ data for a six-tube firing sequence in which the delays have been adjusted to maximize the duration of the summed positive-pressure pulse. As discussed in section 3, continuously shrinking delays are required to achieve this. For this sequence, the intended delays were 2.7, 2.2, 1.6, 1.5, and 0.5 ms between successive detonations; the measured delays were 2.2, 1.5, 1.6, 1.2, and 0.5 ms. The delay times in the linear-sum simulation (dotted curve) were again adjusted to fit the measured delays. With some minor crossovers, $p(t)$ remains essentially positive for 8 ms and then goes strongly negative following the last pulse. The overall pulse train duration is about 15 ms. The spectrum of this pulse train (fig. 14(b) and (c)) shows a large compound peak from 53 to 76 Hz, a

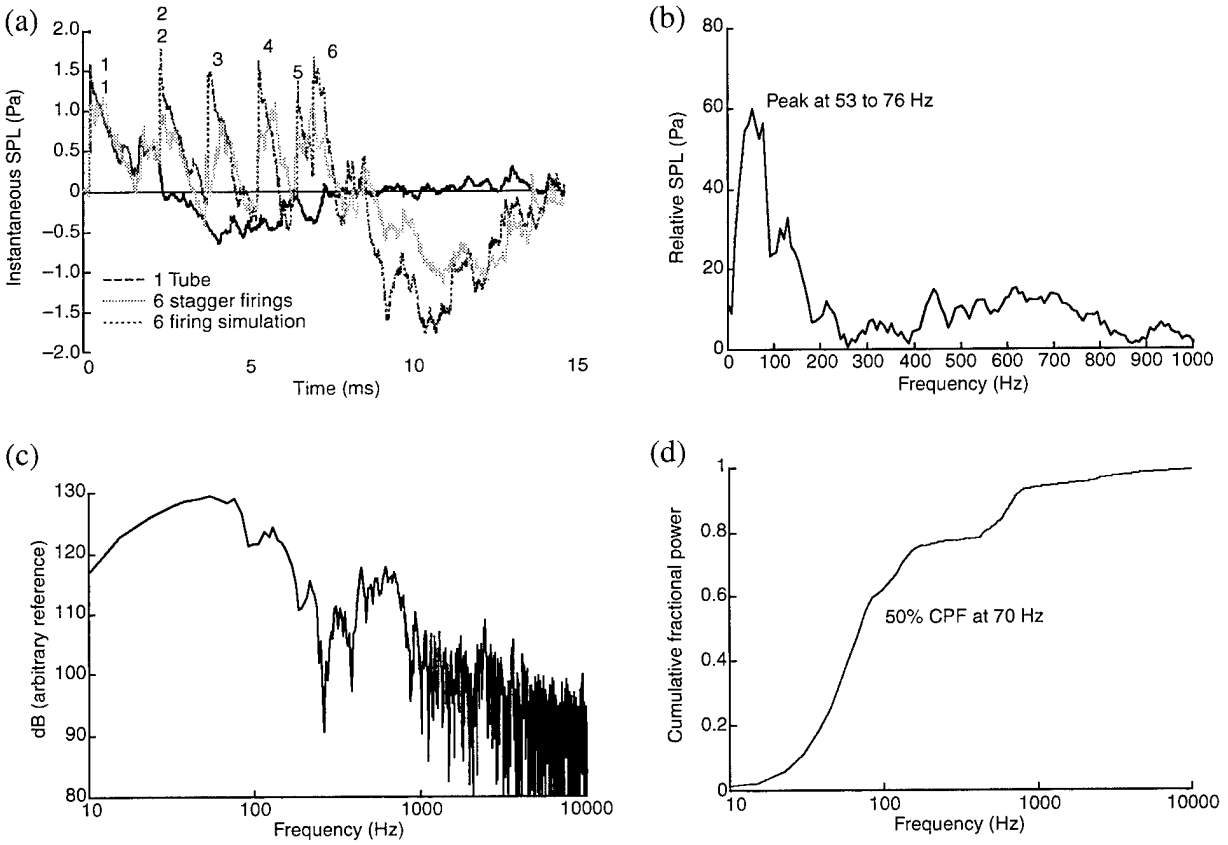

Figure 14. Pulse measured at 15.24 m from six DTs fired with measured Δt_i = 2.2, 1.5, 1.6, 1.2, and 0.5 ms: (a) measured time history of SPL, $p(t)$ (solid curve), and calculated $p(t)$ based on single DT pulse (dotted curve); (b) measured low-frequency acoustic spectrum; (c) logarithmic acoustic spectrum; and (d) integrated fractional acoustic power as a function of frequency.

lesser peak near 125 Hz, and a broad hump from about 400 to 800 Hz. We may identify the 70-Hz peak with the overall pulse duration ($f \sim 1/(15$ ms)), the 125-Hz peak with the positive duration ($f \sim 1/(8$ ms)), and the 400- to 800-Hz hump as the contribution from the pulse delays ($f \sim 1/(2.5$ ms) to $f \sim 1/(1.25$ ms)). For this sequence, the 50 percent CPF value of 70 Hz falls within the frequency range of the 50- to 76-Hz compound spectral peak.

Table 1 summarizes the acoustic spectrum results from the representative measurements. For the 0-, 8-, 5-, and 2.2- to 0.5-ms delay cases, the 50-percent CPF corresponds closely to the frequency of the spectral peak with the greatest amplitude; i.e., the dominant and mean power frequencies tend to be the same. In these sequences, the acoustic power tends to be concentrated near a single frequency. When the dominant and mean power frequencies differ, the acoustic output power tends to be distributed across a broader band of frequencies. The 50-percent CPF is probably the better overall measure of the *effective* frequency of the source, since it properly weights the entire spectrum and is stable with respect to minor spectral shifts. The 2.2- to 0.5-ms delay sequence is most effective at shifting the source spectrum toward lower frequencies, even though the

Table 1. Dominant and mean power frequencies and percent power above 1 kHz from single and multiple detonation tube firings measured at 15.24-m range.

Experiment	Dominant spectrum peak (Hz)	50% cumulative power frequency (Hz)	Percentage of power above 1 kHz
Single tube	92	122	8.5
Six tubes, 0-ms delays	90	88	3.2
Six tubes, 8-ms delays	130	126	5.4
Six tubes, 5-ms delays	200	199	11.8
Six tubes, 4-ms delays	107	244	12.5
Six tubes, 2-ms delays	40	108	12.1
Six tubes, 2.2- to 0.5-ms delays	53–76	70	6.0

DT pulse train used for this sequence has the shortest overall length of those cases examined.

A consistent feature of the spectra of both the single and multiple DT pulses is the –20 dB per decade overall roll-off at frequencies above 1 kHz. Altogether, these spectra may be viewed as a combination of a series of low frequencies that are determined by the characteristics of the individual DT and their firing delays, plus a $1/f$ high-frequency noise component. Table 1 shows the percentage of the measured acoustic power at frequencies above 1 kHz for the DT firings discussed above. The lowest high-frequency content is associated with the six-tube simultaneous-fire sequence. The 8-ms and variable delay sequence resulted in 5 to 6 percent of the energy above 1 kHz; this is not surprising, since these timings either translated the acoustic energy to lower frequencies or concentrated it in a narrow frequency band. The 5- to 2-ms delay sequences show an increased high-frequency content; as noted above, these delays are not efficient at either translating or concentrating the acoustic spectrum.

6. Conclusions

We have measured the pressure-time waveform and frequency content of the acoustic output from single and multiple detonation tubes. We report results for single tubes as a function of range in the moderate-shock to acoustic range (from 1 MPa to below 1 kPa). The variation of the measured overpressures and pulse durations with range are well described by existing models for spherical blast waves if an effective initial radius and initial conditions are assumed near the source. The increase in pulse duration with range accounts well for the measured decrease with range of the mean frequency (50% CPF) of the acoustic power spectrum. At ranges of 0.5 m or greater, the acoustic signal from the shock wave is augmented by a second shock, attributable to supersonic jet formation from the DT. Our experimental results confirmed our hypothesis that the acoustic spectrum from a DT can be shifted to lower frequencies by the timed addition of multiple DT pulses that, in effect, extend the positive-pressure pulse duration. Judicious staggering of multiple pulses produced the largest down-conversion of acoustic energy and resulted in a shift of the median energy from 122 Hz for a single tube to 70 Hz for six tubes with optimal pulse staggering. The results also show that the majority of the source acoustic power can be very effectively concentrated in a narrow frequency band the pulse delays are *tuned* to match the overall duration of an individual pulse.

References

1. L. I. Sedov, *Similarity and Dimensional Methods in Mechanics*, Academic Press, New York (1959).
2. J. W. Reed, "Atmospheric Attenuation of Explosion Waves," *J. Acoust. Soc. Am.* **61** (1977), pp 39–47.
3. I. Kohlberg, H. E. Boesch, Jr., B. T. Benwell, and C. G. Reiff, *Prediction of Successive Radial Shock-on-Shock Interactions Using Thin Shell Model*, submitted for presentation at the 38th AIAA Aerospace Sciences Meeting, Reno, NV (10–13 January 2000).
4. R. Rasp, "Shock Waves, Blast Waves, and Sonic Booms," *Handbook of Acoustics*, M. J. Crocker, ed., J. Wiley & Sons, Inc. New York (1998), p 300.

Distribution

Admnstr
Defns Techl Info Ctr
Attn DTIC-OCP
8725 John J Kingman Rd Ste 0944
FT Belvoir VA 22060-6218

Ofc of the Secy of Defns
Attn ODDRE (R&AT)
The Pentagon
Washington DC 20301-3080

Ofc of the Secy of Defns
Attn OUSD(A&T)/ODDR&E(R) R J Trew
3080 Defense Pentagon
Washington DC 20301-7100

AMCOM MRDEC
Attn AMSMI-RD W C McCorkle
Redstone Arsenal AL 35898-5240

CECOM
Attn PM GPS COL S Young
FT Monmouth NJ 07703

Dir for MANPRINT
Ofc of the Deputy Chief of Staff for Prsnnl
Attn J Hiller
The Pentagon Rm 2C733
Washington DC 20301-0300

TACOM/ARDEC
Attn AMSTA-AR-CCL-E C Freund
Attn AMSTA-AR-QAC K Yagrich
Attn AMSTA-AR-QAC T Hartmann
Attn AMSTA-AR-CCL-D H Moore
Picatinny Arsenal NJ 07806

US Army ARDEC
Attn AMSTA-AR-TD M Fisette
Bldg 1
Picatinny Arsenal NJ 07806-5000

US Army Info Sys Engrg Cmnd
Attn ASQB-OTD F Jenia
FT Huachuca AZ 85613-5300

US Army Natick RDEC Acting Techl Dir
Attn SSCNC-T P Brandler
Natick MA 01760-5002

US Army Simulation, Train, & Instrmntn Cmnd
Attn J Stahl
12350 Research Parkway
Orlando FL 32826-3726

US Army Soldier & Biol Chem Cmnd
Dir of Rsrch & Techlgy Dirctrt
Attn SMCCR-RS I G Resnick
Aberdeen Proving Ground MD 21010-5423

US Army Tank-Automtv Cmnd Rsrch, Dev, & Engrg Ctr
Attn AMSTA-TR J Chapin
Warren MI 48397-5000

US Army Train & Doctrine Cmnd
Battle Lab Integration & Techl Dirctrt
Attn ATCD-B J A Klevecz
FT Monroe VA 23651-5850

Nav Surface Warfare Ctr
Attn Code B07 J Pennella
17320 Dahlgren Rd Bldg 1470 Rm 1101
Dahlgren VA 22448-5100

DARPA
Attn S Welby
3701 N Fairfax Dr
Arlington VA 22203-1714

Hicks & Associates Inc
Attn G Singley III
1710 Goodrich Dr Ste 1300
McLean VA 22102

Director
US Army Rsrch Ofc
Attn AMSRL-RO-D JCI Chang
PO Box 12211
Research Triangle Park NC 27709

US Army Rsrch Lab
Attn AMSRL-DD J M Miller
Attn AMSRL-CI-AI-A Mail & Records Mgmt
Attn AMSRL-CI-AP Techl Pub (3 copies)
Attn AMSRL-CI-LL Techl Lib (3 copies)
Attn AMSRL-SE-DE C Reiff (5 copes)

Distribution (cont'd)

US Army Rsrch Lab (cont'd)
Attn AMSRL-SE-DS E Boesch Jr (20 copies)
Attn AMSRL-SE-DS J Tatum

US Army Rsrch Lab (cont'd)
Attn AMSRL-SE-DS L Jasper
Adelphi MD 20783-1197

REPORT DOCUMENTATION PAGE

Form Approved
OMB No. 0704-0188

1. AGENCY USE ONLY *(Leave blank)*	2. REPORT DATE	3. REPORT TYPE AND DATES COVERED
	May 2000	Final, 1/98–12/99

4. TITLE AND SUBTITLE Modification of the Acoustic Spectrum of Detonation Tube Shock Waves by Timed Multiple-Pulse Addition

5. FUNDING NUMBERS
DA PR: A140
PE: 62120A

6. AUTHOR(S) H. Edwin Boesch, Jr., Christian G. Reiff (ARL), Bruce T. Benwell (Directed Energy Technologies)

7. PERFORMING ORGANIZATION NAME(S) AND ADDRESS(ES)
U.S. Army Research Laboratory
Attn: AMSRL-SE-DS email: eboesch@arl.mil
2800 Powder Mill Road
Adelphi, MD 20783-1197

8. PERFORMING ORGANIZATION REPORT NUMBER
ARL-TR-2203

9. SPONSORING/MONITORING AGENCY NAME(S) AND ADDRESS(ES)
U.S. Army Research Laboratory
2800 Powder Mill Road
Adelphi, MD 20783-1197

10. SPONSORING/MONITORING AGENCY REPORT NUMBER

11. SUPPLEMENTARY NOTES
ARL PR: 0NEYYY
AMS code: 622120.140

12a. DISTRIBUTION/AVAILABILITY STATEMENT Approved for public release; distribution unlimited.

12b. DISTRIBUTION CODE

13. ABSTRACT *(Maximum 200 words)*

Detonation tubes are simple devices capable of producing substantial acoustic power that may be useful for the simulation of high-level acoustic environments. We report results of an investigation into the modification of the acoustic spectrum produced by detonation tubes by timed addition of the shock-wave outputs of six detonation tubes fired in sequence. We first examined the output of a single detonation tube as a function of range and found that it conformed to existing models for spherical blast waves when appropriate initial conditions were derived. We found timing schemes for the firing of the multiple tubes that (1) produce a substantial shift of the acoustic energy to lower frequencies by maximizing the duration of the positive pressure pulse, or (2) maximize the acoustic energy output in a narrow frequency range by matching the pulse-to-pulse delay to the total duration (positive and negative pressure phases) of a single detonation wave.

14. SUBJECT TERMS
Shock wave, blast wave

15. NUMBER OF PAGES
31

16. PRICE CODE

17. SECURITY CLASSIFICATION OF REPORT	18. SECURITY CLASSIFICATION OF THIS PAGE	19. SECURITY CLASSIFICATION OF ABSTRACT	20. LIMITATION OF ABSTRACT
Unclassified	Unclassified	Unclassified	SAR

NSN 7540-01-280-5500

Standard Form 298 (Rev. 2-89)
Prescribed by ANSI Std. Z39-18
298-102